

Quasi-2D Behavior in Bulk Isotropic Type-II Superconductors: Shape Effects

F. Hellman,⁽¹⁾ E. M. Gyorgy,⁽²⁾ and R. C. Dynes⁽¹⁾

⁽¹⁾University of California at San Diego, La Jolla, California 92093

⁽²⁾AT&T Bell Laboratories, Murray Hill, New Jersey 07974

(Received 24 April 1991)

The induced magnetization of an isotropic type-II superconductor with an anisotropic sample shape has been measured in an oblique magnetic field and separated into its reversible and irreversible contributions. The measurements unexpectedly show that the irreversible magnetization is oriented essentially parallel to the smallest sample dimension, and is almost independent of the angle of the applied field. This behavior can be understood by considering the critical-state model when the applied field is at an arbitrary direction with respect to the sample axes.

PACS numbers: 74.60.Ge, 74.30.Ci

Much recent work has focused on the anomalous effects of a magnetic field applied at an angle to the a - b planes of the anisotropic high- T_c copper oxide superconductors [1-7]. Observed anisotropy in the irreversible (pinned) behavior is interpreted as being due to the intrinsic anisotropy of the material [1-5]. We have found, however, that when vortex pinning is present, even isotropic type-II superconductors exhibit unexpected results which can be explained as being due purely to sample *shape* considerations. For bulk parallelepipeds with geometrical aspect ratios as low as 2:1, the irreversible magnetization is oriented essentially parallel to the smallest dimension and does not change as the angle of the applied field is varied from perpendicular to greater than a 45° angle. This unexpected observation is shown here to result from the Bean critical-state model [8] modified to include an applied field at an angle with respect to the sample axes.

The measurements were made on polycrystalline Nb and Pb-Bi alloys. The applied field H_a was cycled between H_{c2} and $-H_{c2}$. The induced magnetization density \mathbf{M} , due to the macroscopic screening currents, was measured using a vibrating sample magnetometer to determine the component of \mathbf{M} along H_a , M_{VSM} , and a torque magnetometer to determine the component of \mathbf{M} perpendicular to H_a , M_{tor} . All measurements were made at 4.2 K.

There are two contributions to \mathbf{M} : (a) a reversible part \mathbf{M}_r due to a screening current near the sample surface and associated with the expulsion of the magnetic field, and (b) an irreversible part \mathbf{M}_i associated with pinning of the vortices and the resultant vortex density gradient and screening current throughout the sample. The reversible contribution below H_{c1} equals $-H/4\pi$ (the usual Meissner effect) and above H_{c1} is determined by the repulsive interactions of the vortices [9,10]. Demagnetization corrections due to geometry increase the absolute value of the initial slope above $1/4\pi$ and cause \mathbf{M}_r to lie along a direction different from H_a [9-11]. The irreversible contribution results from pinning of the vortices as they attempt to enter or leave the sample (in increasing or decreasing applied fields, respectively). A critical state is

set up in which a vortex density gradient and a concomitant critical current J_c flows throughout the sample, resulting in a magnetization M_i [8,12]. The sign of the gradient, the direction of the current flow, and hence the sign of M_i depend on whether H_a is increasing or decreasing. J_c and hence M_i depend on the magnitude of the field. The angle of \mathbf{M}_i relative to H_a has not been considered previously.

We first demonstrate the separation of the reversible and irreversible components from the measured magnetization. The reversible contribution is determined by taking $M_r(H) = [M(H_{decr}) + M(H_{incr})]/2$. The irreversible contribution is $M_i(H) = [M(H_{decr}) - M(H_{incr})]/2$. Figure 1 shows this separation for a sample of Nb $2 \times 1 \times 10$ mm³ in an applied field perpendicular to the 2×10 face. When the field is perpendicular to one of the faces, \mathbf{M} is purely along H_a . For angles of H_a other than 90° and 0° , \mathbf{M} is at a different angle and hence $M_{tor} = \tau/H_a$ (where $\tau = |\mathbf{M} \times H_a|$) is needed. The reversible contribution \mathbf{M}_r is then given by a magnitude $|\mathbf{M}_r| = (M_{r(tor)}^2 + M_{r(VSM)}^2)^{1/2}$ and an angle α_r where $\tan(\theta - \alpha_r) = M_{r(tor)}/M_{r(VSM)}$. α_r and θ are the angles of \mathbf{M}_r and

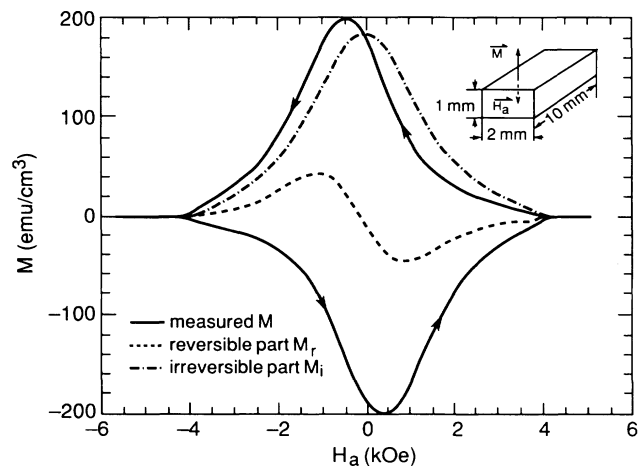


FIG. 1. Magnetic moment vs H_a for $2 \times 1 \times 10$ -mm³ Nb; H_a normal to 2×10 face. The full moment, reversible, and irreversible components are shown.

H_a , respectively, measured from the sample normal. The irreversible contribution \mathbf{M}_i is similarly defined.

We first consider the initial magnetization after cooling in zero field. This magnetization is fully reversible up to a well-defined field equal to the demagnetized value of H_{c1} . For all samples, the angle and magnitude of \mathbf{M} agree precisely with that expected from the Meissner state with appropriate demagnetization factors [13].

After cycling above H_{c2} , \mathbf{M}_r contains a more complicated demagnetization factor, as the total value of \mathbf{M} contributes to the demagnetizing field. This demagnetizing field will also separate into reversible and irreversible contributions, but due to the nonlinearity of M_r with H above H_{c1} , this separation is not sufficient to recover the exact dependence of M_r on H_a . In addition, the Meissner screening current will either add to or subtract from the irreversible screening currents over a penetration depth, depending on whether H_a is increasing or decreasing. This second factor causes a reduction in the measured value for M_r and for the slope dM_r/dH_a (relative to the Meissner state) even when demagnetizing is negligible. In spite of these complications, the thermodynamic relationship $\int_0^{H_{c2}} M_r dH_a = H_c^2/8\pi$ must hold [10]. We have indeed found that for all angles θ this integral gives a value for H_c of 1480 ± 20 Oe. This value is in agreement with accepted values for Nb [14], giving us confidence that this separation into reversible (intrinsic magnetization) and irreversible (pinning) contributions is valid.

We turn now to the irreversible component. Since \mathbf{M}_i is the result of screening currents throughout the sample, unlike \mathbf{M}_r , a simple demagnetizing factor does not exist; instead the self-field must be numerically calculated [12]. Quantitative analysis of \mathbf{M}_i is only valid for $H_a > 2$ kOe where the self-field is negligible. However, comparisons of \mathbf{M}_i for different θ are meaningful at all H_a . Figure 2 shows \mathbf{M}_i for the $1 \times 1 \times 10\text{-mm}^3$ sample. For $\theta = 0^\circ, 45^\circ,$

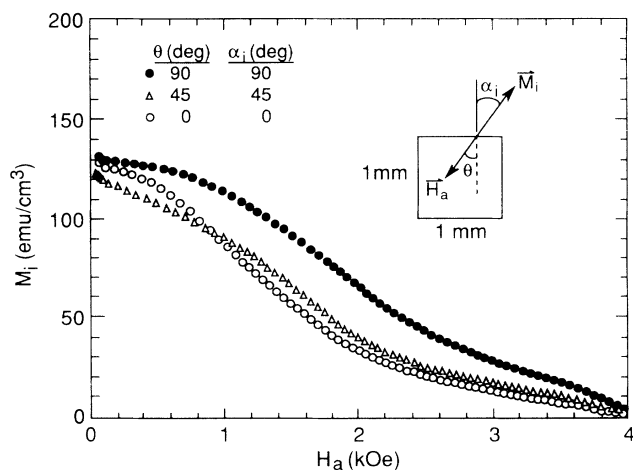


FIG. 2. M_i vs H_a for $1 \times 1 \times 10\text{-mm}^3$ Nb for various θ . For $\theta = 45^\circ$, M_i has been divided by 0.94 to normalize to $\theta = 90^\circ$ data [15]. The angle α_i is shown in the inset.

and 90° , \mathbf{M}_i is parallel to \mathbf{H}_a : $\alpha_i = \theta$. The magnitude is as expected [15]; the curves are similar to each other but do exhibit a systematic variation. This is a consequence of metallurgical anisotropy in the sample; J_c perpendicular to the original roll direction of the material differs slightly from J_c in the plane parallel. This small difference will not affect our conclusions, and, in fact, can be used to strengthen them, as we discuss later.

Figure 3 shows the magnitude and angle of \mathbf{M}_i for the $2 \times 1 \times 10\text{-mm}^3$ sample. Unlike the $1 \times 1 \times 10\text{-mm}^3$ sample, \mathbf{M}_i is now virtually perpendicular to the 2×10 face for $\theta = 22.5^\circ$ and even 45° ($\alpha_i \approx 6^\circ$). At $\theta = 67.5^\circ$, \mathbf{M}_i falls away from perpendicular ($\alpha_i \approx 35^\circ, \alpha_r \approx 40^\circ - 50^\circ$) and is in-plane for $\theta = 90^\circ$, as it must be from symmetry. The 90° and 0° data are almost identical to the results on the $1 \times 1 \times 10\text{-mm}^3$ sample, showing the same metallurgical consequences. For $\theta = 22.5^\circ$ and 45° , \mathbf{M}_i is nearly identical in all respects to the values at $\theta = 0^\circ$. Therefore, the shielding currents producing \mathbf{M}_i must be closely relat-

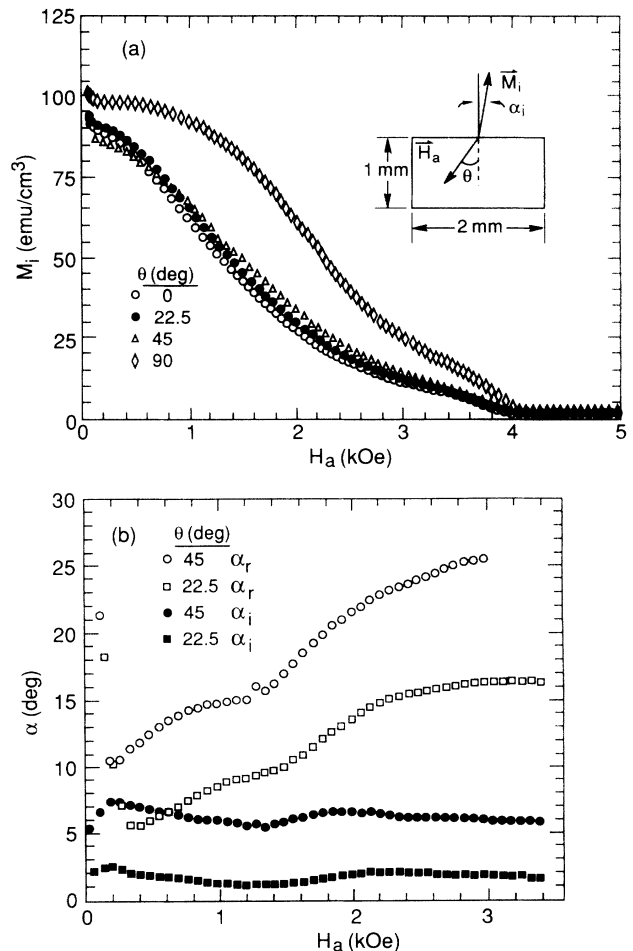


FIG. 3. (a) M_i vs H_a for $2 \times 1 \times 10\text{-mm}^3$ Nb for various θ . M_i has been divided by 2 for $\theta = 0^\circ, 22.5^\circ,$ and 45° to normalize to $\theta = 90^\circ$ data since $\alpha_i \approx 0^\circ$ for these θ . (b) α_r and α_i vs H_a for $\theta = 22.5^\circ$ and 45° .

ed for these three angles. The metallurgically induced difference in J_c vs H_a for $\theta=0^\circ$ and 90° further emphasizes that the induced current pattern is virtually identical at $\theta=0^\circ, 22.5^\circ,$ and 45° .

A thinner $2 \times 0.127 \times 10\text{-mm}^3\text{-Nb}$ and a Pb-2-at.\%Bi alloy sample show similar behavior. \mathbf{M}_i is within 5° of perpendicular for all θ (except 90°), including 67.5° . A Pb-0.5-at.\%Bi sample (type-I superconductor) was also measured. For both Pb-Bi alloys, the integral of M_r gave an H_c of 550 Oe, as expected [16,17].

We note that these effects are not due to any surface or anomalous metallurgical effect (such as oriented pinning sites), as the $1 \times 1 \times 10\text{-mm}^3$ sample was cut from the same bulk specimen and exhibits no such anomalous behavior. Furthermore, both Nb and Pb-Bi show the same effects, despite different vortex pinning strength. As an additional test, we annealed the $2 \times 1 \times 10\text{-mm}^3\text{-Nb}$ sample in O_2 at 400°C for 5 min, a well-known recipe for reducing surface pinning effects [18], and found no significant changes.

To understand the experimental results, we consider the Bean critical-state model for a rectangular parallelepiped $a \times b \times L$ with $L \gg a$ and b and the z axis along L . \mathbf{H}_a is at an angle to the sample axes, in the x - y plane. H_a is assumed to be large compared to the self-field due to the induced currents. The origin of the coordinate system is at the center of the sample. The current distribution at $z=0$ is shown in Fig. 4 for two values of θ . For H_a decreasing, current with density J_c flows along $+z$ (out of the page) to the left of the line AB and along $-z$ to the right of AB . The vortices enter at points C and D and are parallel to \mathbf{H}_a (since the self-field is small in this high-field limit). The figure shows three separate regions: unshaded (white), hatched, and cross hatched. The current distribution everywhere except the two small cross-hatched regions is identical to that for $\theta=0^\circ$.

The total magnetic moment can be obtained from

$$\mathbf{m} = \frac{1}{2} \int \mathbf{r} \times \mathbf{J} dV,$$

where $\mathbf{J} = J_c$ and V is the volume. This equation shows

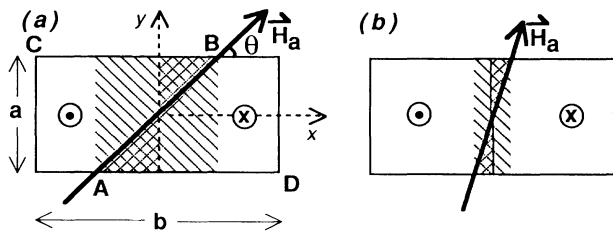


FIG. 4. Cross section of the sample at $z=0$. Applied field at (a) $\theta=45^\circ$ and (b) $\theta=15^\circ$. For H_a decreasing, the current flows out of the page (\odot) to the left of the line AB and into the page (\otimes) to the right. Vortices enter at points C and D . Cross hatching shows regions where current flows oppositely for $\theta=0^\circ$ vs $\theta \neq 0^\circ$. Shaded and unshaded regions are used to calculate the moment.

the relative unimportance of the cross-hatched region since r is smallest here. Thus, qualitatively, it may already be seen that the current pattern shown in Fig. 4 will give an angle α_i of \mathbf{M}_i which is near zero for most θ . It is also readily seen that as the aspect ratio a/b decreases, the effect of the cross-hatched region will decrease still further, causing $\alpha_i \rightarrow 0^\circ$. Thus even relatively thick samples will mimic 2D behavior.

It is straightforward to calculate \mathbf{m} for arbitrary θ for the current distribution shown in Fig. 4. This calculation leads to \mathbf{m} nearly perpendicular as expected. However, the "closure" currents at the ends of the sample ($z \approx \pm L/2$) are more complicated. Since in the Bean model all current densities are equal to J_c , current conservation requires a "mapping" of points on the left of line AB to points on the right. The current from the outer, unshaded region must flow parallel to the x axis around the end of the sample ($z \approx \pm L/2$), while that in the shaded regions (comprising both hatched and cross-hatched regions) flows closer to the middle (smaller $|z|$) at an angle to the x and y axes. For angles of θ other than 45° , attempts to connect points on either side of line AB [see Fig. 4(b)] will quickly convince the reader that the closure currents for the shaded regions will not be uniform in direction. While a precise calculation of the angle of \mathbf{J}_c in these closure currents, and hence their contribution to \mathbf{m} for arbitrary θ , is beyond the scope of this paper, the largest contribution (largest $r \approx \pm L/2$) is from currents due to the unshaded region. These lie in the plane (along x), again leading to \mathbf{m} nearly perpendicular.

For purposes of illustration, we restrict ourselves here to the simplest case of the $2 \times 1 \times 10\text{-mm}^3$ sample with the applied field at 45° [Fig. 4(a)]. In this case, the shaded regions make a $1 \times 1 \times 10\text{-mm}^3$ bar and the unshaded region is a $2 \times 1 \times 10\text{-mm}^3$ rectangular toroid with wall thickness 0.5 mm. The closure current from the shaded regions near $z \approx \pm L/2$ will flow perpendicular to \mathbf{H}_a . This current pattern is identical to a $1 \times 1 \times 10\text{-mm}^3$ sample with \mathbf{H}_a at 45° . The moment \mathbf{m}_s of these shaded regions is at 45° with a magnitude $m_s = \sqrt{2} a^3 L J_c / 60$ [15]. The closure current from the unshaded region must flow parallel to the x axis. This current distribution is that of a rectangular toroid with \mathbf{H}_a at 0° and produces a moment \mathbf{m}_u at 0° with magnitude $m_u = (J_c/40)(4a^3 L - a^3 L) = 3a^3 L J_c / 40$ ($a=0.1$ cm) [15]. Then the total moment is at an angle $\alpha_i = \tan^{-1}[m_s \sin 45^\circ / (m_s \cos 45^\circ + m_u)] = 10^\circ$, in agreement with results shown in Fig. 3(b) and far smaller than the 27° found for the Meissner state [13]. The total magnetic moment is 93% of that obtained for $\theta=0^\circ$, again in good agreement with the measurements. Note that the angle of α_i should be independent of H_a , as observed: The magnitude of J_c and hence \mathbf{M}_i will go to zero at H_{c2} , but the current pattern shown in Fig. 4 and hence α_i will not change. By contrast, α_r depends strongly on H_a both theoretically [11] and exper-

imentally. The observation that α_i is essentially independent of H_a even at low applied fields indicates that the current distribution shown in Fig. 4 is apparently valid for lower values of the applied field than might be expected.

In conclusion, we have measured the reversible and irreversible contributions to the magnetization induced by an applied field in an isotropic type-II superconductor. From the reversible part, we are able to obtain the thermodynamic critical field H_c at the measurement temperature. For the irreversible part, with H_a at an arbitrary angle, we have presented a modified current distribution for the Bean critical-state model that well accounts for the unexpected observation that the resulting irreversible magnetization lies essentially along the sample normal even for aspect ratios as low as 2:1. We have demonstrated these effects in a slab geometry, but analogous effects will be seen in all geometries. Since anisotropic materials such as the high- T_c superconductors frequently possess a plate geometry, these results indicate that interpretations [1-5] of their irreversible magnetic behavior in terms of an intrinsic material anisotropy may need to be reexamined.

We thank J. R. Clem, R. B. van Dover, and especially V. G. Kogan for valuable discussions. This work was partially supported by AFOSR Grant No. 89-0432 and the Universitywide Energy Research Group Program.

-
- [1] I. Felner, U. Yaron, Y. Yeshuran, G. V. Chandrashekar, and F. Holtzberg, *Phys. Rev. B* **40**, 5239 (1989).
 - [2] W. Andrä, H. Danan, and R. Hergt, *Phys. Status Solidi* **111**, 583 (1989).
 - [3] L. Fruchter, C. Aguilon, S. Senoussi, and I. A. Campbell, *Physica (Amsterdam)* **160C**, 185 (1989).
 - [4] H. Teshima, A. Oishi, H. Izumi, K. Ohata, T. Morishita, and S. Tanaka, *Appl. Phys. Lett.* **58**, 2833 (1991).
 - [5] D. Feinberg and C. Villard, *Phys. Rev. Lett.* **65**, 919

- (1990).
- [6] C. A. Bolle, P. L. Gammel, D. G. Grier, C. A. Murray, D. J. Bishop, D. B. Mitzi, and A. Kapitulnik, *Phys. Rev. Lett.* **66**, 112 (1991).
- [7] D. E. Farrell, J. P. Rice, D. M. Ginsberg, and J. Z. Liu, *Phys. Rev. Lett.* **64**, 1573 (1990).
- [8] Charles P. Bean, *Rev. Mod. Phys.* **36**, 31 (1964).
- [9] M. Tinkham, *Introduction to Superconductivity* (McGraw-Hill, New York, 1980).
- [10] A. Fetter and P. Hohenberg, in *Superconductivity*, edited by R. D. Parks (Dekker, New York, 1969).
- [11] J. A. Cape and J. M. Zimmerman, *Phys. Rev.* **153**, 416 (1967); J. A. Cape, *Phys. Rev.* **179**, 485 (1969).
- [12] M. Däumling and D. C. Larbalestier, *Phys. Rev. B* **40**, 9350 (1989).
- [13] We assume, for example, a $1 \times 2 \times 10$ -mm³ parallelepiped to be an ellipsoid with demagnetizing factors $D_i = \frac{1}{3}, \frac{2}{3}$, and 0. \mathbf{M} is calculated by setting $\mathbf{B}=0$ inside the slab and using the appropriate x and y components of \mathbf{M} , \mathbf{H}_a , \mathbf{H}_{int} , and D . With the coordinate system of Fig. 4, $\tan\alpha = [(1 - D_x)/(1 - D_z)] \tan\theta$. For $\theta = 45^\circ$, $\alpha = 27^\circ$. See also Ref. [11].
- [14] T. McConville and B. Serin, *Phys. Rev.* **140**, A1169 (1965). $H_c(4.2 \text{ K}) = 1550 \text{ Oe}$.
- [15] In the Bean critical-state model, a sample $t \times w \times L$ with $L \gg w$ and \mathbf{H}_a perpendicular to the $L \times w$ face has moment $m \sim J_c w^2 L t / 40$ (units of G, cm, and A) [8]. For a sample $a \times a \times L$ ($L \gg a$) with \mathbf{H}_a perpendicular to L and at 45° to the $a \times L$ face, the magnetization \mathbf{m} will be parallel to \mathbf{H}_a and $m = 2 \int dm$, where $dm = (J_c w^2 L / 40) dt$ is the moment for a slab of infinitesimal thickness dt , width $w = a\sqrt{2} - 2t$, and length L . The integral is from $t = 0$ to $a\sqrt{2}/2$. Then $m = \sqrt{2} a^3 J_c / 60$, 0.94 of the value for H_a normal.
- [16] R. C. Dynes and J. M. Rowell, *Phys. Rev. B* **11**, 1884 (1975).
- [17] C. Kittel, *Introduction to Solid State Physics* (Wiley, New York, 1971), 4th ed., p. 339; *ibid.* (Wiley, New York, 1976), 5th ed., p. 363.
- [18] H. R. Kercher, D. K. Christen, and S. T. Sekula, *Phys. Rev. B* **21**, 86 (1980).